Supporting Information

Zhou and Meier 10.1073/pnas.1323104111

SI Methods

Plant Materials. *Arabidopsis* (Columbia ecotype) plants were grown at 25 °C in soil under 16 h of light and 8 h of dark or on Murashige Skoog Medium (Caisson Laboratories) with 1% sucrose plates under constant light. *WPP domain-interacting tail-anchored protein 1-1* (*wit1-1*) *wit2-1* double null was reported by Zhao et al. (1), and *WPP domain-interacting protein 1-1* (*wip1-1*) *wip2-1 wip3-1* triple null (*wip123*) was reported by Xu et al. (2). Crosses between these two mutants were performed to obtain the quintuple null mutant *wip1-1 wip2-1 wip3-1 wit1-1 wit2-1* mutant. *kaku1-4* (SALK_082443C) was reported by Tamura et al. (3), and the seeds were obtained from the *Arabidopsis* Biological Resource Center.

Constructs. The hygromycin B resistance cassette was amplified by PCR from the vector pH2GW7 (4) using 5′-AATGAATTCATCAGCTTGCATGCCGGTCGATC-3′ and 5′-GCTGAATTCATCATACATGAGAATTAAGGGAGTC-3′ (the EcoRI site is underlined), digested by EcoRI, and then ligated with the EcoRI-digested binary vector pPZP-RCS2 (5). After confirmation by sequencing, the pPZP-RCS2-Hyg vector was obtained. The GFP-gateway-35ST (35S terminator of Cauliflower Mosaic Virus) cassette was amplified by PCR using 5′-TATGGCGCGCCACGTGAGCAAGGGCGAGGAGCTGTTC-3′ (the AscI site is underlined) and 5′-CCGGGGATCCTCTAGAGGGCC-3′ (the XbaI site is underlined), digested by AscI and XbaI, and ligated with the AscI/XbaI-digested pPZP-RCS2-Hyg. After confirmation by sequencing, the pHOAG vector was obtained.

The *WIT1* promoter sequence (~2.1 kb upstream of the start codon of *WIT1*) was amplified by PCR from *Arabidopsis* (ecotype Columbia) DNA using 5′-ATCGAGCTCCAATGGGTCCTGTGTTGGTCCACG-3′ (SacI site is underlined) and 5′-CATCTTTCAATATAACTGCAACAGAGAAAGTA-3′, digested by SacI, and ligated with the SacI/PmlI-digested pHOAG. After sequencing, the pHWIT1proAG vector was obtained. *WIT1* coding sequence cloned in pENTR/D-TOPO vector (Life Technologies) was described by Zhao et al. (1) and moved to pHWIT1proAG by an LR reaction (Life Technologies) to obtain the *WIT1pro::GFP-WIT1* construct. The *WIP1* promoter (~2.6 kb upstream of the start codon of *WIP1*) was amplified by PCR from *Arabidopsis* DNA using 5′-GGAAGGCGCGCCCACCGTTATGACTCG-3′ (AscI site is underlined) and 5′-CATTGACTCCACAAAAAAATCTATC-3′, digested by AscI, and ligated with the AscI/PmlI-digested pHOAG. After confirmation by sequencing, the pHWIP1proAG vector was obtained. *WIP1* coding sequence cloned in pENTR/D-TOPO vector was described by Xu et al. (2) and moved to pHWIP1proAG by an LR reaction to obtain the *WIP1pro::GFP-WIP1* construct.

To clone *Ran GTPase activating protein 1* (*RanGAP1pro::RanGAP1-GFP*), the pK7FWG2 vector (4) was digested with SpeI and HindIII to remove Cauliflower Mosaic Virus 35S promoter. Phusion DNA polymerase (New England Biolabs) was used to fill the sticky ends of the digested vector, and the linear vector was circularized using T4 DNA ligase (New England Biolabs) to obtain the pK7FWG vector. *RanGAP1pro::RanGAP1* was amplified by PCR from *Arabidopsis* genomic DNA using 5′-GGGGACAAGTTTGTACAAAAAAGCAGGCTTTctccaacgaatctgcaatg-3′ and 5′-GGGGACCACTTTGTACAAGAAAGCTGGGTATTCCTCCCCTTGCTTG-3′ and cloned to pDONR221 using BP reaction (Life Technologies). After sequencing, the RanGAP1pro::RanGAP1 fragment was moved to pK7FWG by LR reaction (Life Technologies) to obtain the RanGAP1pro::RanGAP1-GFP construct.

The following steps were performed to clone the Egg Cell 1 promoter-driven nuclear localization signal fused double red fluorescent proteins (*EC1pro::NLS-2xRFP*) construct. The Kanamycin resistance cassette was amplified by PCR from the vector pK7WGF2 (4) using 5′-AATGAATTCATCAGCTTGCATGCCGGTCGATC-3′ and 5′-GCTGAATTCATCATACATGAGAATTAAGGGAGTC-3′ (the EcoRI site is underlined), digested by EcoRI, and then ligated with the EcoRI-digested binary vector pPZP-RCS2 (5). After confirmation by sequencing, the pPZP-RCS2-Kan vector was obtained. The pH7RWG2 vector was digested with XbaI and SpeI. The fragment containing the Gateway-RFP cassette was recovered and ligated to XbaI-digested pPZP-RCS2-Kan vector to obtain the pKAR vector. *EC1pro* was amplified by PCR from *Arabidopsis* genomic DNA using 5′-CACCACGGAATTAGCATATCTCATGCACG-3′ and 5′-TCTACCTTTCTCTTCTTTTTTGGCATTTCTCAACAGATTGATAAGGTCGA-3′. *NLS-RFP* was amplified from pH7RWG2 by overlapping PCR using 5′-AGGTAGAAGACCCCGGATCAGGTGGAGGTTCAATGGCCTCCTCCGAGGAC-3′, 5′-TGCCAAAAAAGAAGAGAAAGGTAGAAGACCCCGGATCAGGTGGAGGTTCA-3′, and 5′-GGCGCCGGTGGAGTGGCG-3′. EC1pro::NLS-RFP was amplified by overlapping PCR using the *EC1pro* and the *NLS-RFP* as templates and the following primers: 5′-CACCACGGAATTAGCATATCTCATGCACG-3′ and 5′-GGCGCCGGTGGAGTGGCG-3′. The *EC1pro::NLS-RFP* PCR product was cloned to pENTR/D-TOPO vector (Life Technologies). After sequencing, *EC1pro::NLS-RFP* was moved to pKAR to obtain the *EC1pro::NLS-2xRFP* construct.

Generation of Transgenic Plants. Binary constructs were transformed to *Agrobacterium* strain ABI by triparental mating (6). The *vegetative nucleus-RFP*, *sperm cell nuclei-GFP* marker, and Lat52 promoter-driven GFP (Lat52pro::GFP) marker *Agrobacterium* strains and the WT *Arabidopsis* line transformed with these markers were gifts from R. Keith Slotkin, The Ohio State University, Columbus, OH. *Lat52pro::DsRed qrt1 Arabidopsis* was a gift from Anna Dobritsa, The Ohio State University, Columbus, OH. Other transgenic *Arabidopsis* lines were obtained by *Agrobacterium*-mediated floral dip (7).

Hoechst 33342 Staining. For Hoechst 33342 staining, a 4% (wt/vol) paraformaldehyde solution containing 4 μM Hoechst 33342 was used to stain pollen grains for at least 20 min. After brief centrifugation and rinsing in PBS buffer (137 mM NaCl, 2.7 mM KCl, 10 mM Na_2HPO_4, 2 mM KH_2PO_4, pH 7.4), pollen grains were mounted in PBS buffer and viewed under a Nikon C90i microscope. The UV-2E/C filter cube (Nikon) was used for imaging. Images were taken using a Nikon DS-Qi1Mc digital camera.

Alexander Staining. Alexander pollen staining was performed as described previously (8).

Pollen Germination Assay. For in vitro germination, pollen grains from the stamens of fully opened flowers were germinated on a pollen germination medium containing 18% (wt/vol) sucrose, 0.01% boric acid, 1 mM $CaCl_2$, 1 mM $Ca(NO_3)_2$, 1 mM $MgSO_4$, and 0.5% agar. Several stage 14 WT or *male sterility 1* (*ms1*) stigmas were placed adjacent to pollen grains to stimulate pollen germination (9, 10). For semi-in vitro pollen germination, stage 14 *ms1* stigmas were saturated with pollen and incubated on the pollen germination medium.

Pollen Tube Nuclear Movement, Length Measurement, and Kymograph Generation. A Nikon Eclipse C90i confocal microscope with minimum or medium aperture was used to collect images. For time course imaging of pollen tube growth, a *z*-stack (step size is 5 μm) was taken every 1 min for 180 min. To maximize imaging speed, sequential imaging of GFP and RFP was not used, because the vegetative nucleus and sperm cell nuclei can be easily distinguished by their size and shape.

Each channel of the pollen tube growth movie was first split in ImageJ. For every time point, the *z* stack was merged into one frame using maximum projection. The GFP, RFP, and the transmitted light channels were then combined to one RGB color movie. If position shifting occurs, the StackReg plugin with the translation algorithm was used to correct the shift. Length was then measured using ImageJ. Kymographs were generated in ImageJ by first drawing a selection segmented line over the pollen tube growth track and then reslicing the stacks.

Reciprocal Cross and Pollen Competition Assay. Stage 12 stigmas were emasculated and allowed 2 d to develop to stage 14 stigmas, which were hand-pollinated with the pollen of interest. For the pollen competition assay, each one-half of a stage 14 stigma was saturated with the pollen of interest.

Ovule Imaging and Pollen Tube Aniline Blue Staining. A magnifier was used to identify opening flowers with protruding unpollinated stigmas (early stage 13) (11). These flowers were marked, and the ovaries from these flowers were collected 72 h later. For imaging ovules, ovaries were dissected, and ovules were mounted in 80 mM Sorbitol for confocal microscopy. To image embryos in fertilized ovules, ovules were treated with 8 M NaOH overnight before being mounted in water for imaging. For aniline blue staining, ovaries were fixed in a solution containing acetic acid and ethanol (vol/vol = 1/3) for 2 h, washed in a 70%, 50%, 30%, and 0% (vol/vol) ethanol gradient for 10 min each time, and softened in 8 M NaOH overnight. Aniline blue solution containing 0.1% (wt/vol) aniline blue and 108 mM K_3PO_4 (pH 11) was decolorized by running through activated carbon powder and used to stain the softened ovaries for more than 24 h. Stained ovaries were dissected, and ovules were imaged using a Nikon C90i microscope equipped with a UV-2A filter cube (Nikon) and a Nikon DS-Qi1Mc digital camera.

1. Zhao Q, Brkljacic J, Meier I (2008) Two distinct interacting classes of nuclear envelope-associated coiled-coil proteins are required for the tissue-specific nuclear envelope targeting of *Arabidopsis* RanGAP. *Plant Cell* 20(6):1639–1651.
2. Xu XM, Meulia T, Meier I (2007) Anchorage of plant RanGAP to the nuclear envelope involves novel nuclear-pore-associated proteins. *Curr Biol* 17(13):1157–1163.
3. Tamura K, et al. (2013) Myosin XI-i links the nuclear membrane to the cytoskeleton to control nuclear movement and shape in *Arabidopsis*. *Curr Biol* 23(18):1776–1781.
4. Karimi M, Inzé D, Depicker A (2002) GATEWAY vectors for *Agrobacterium*-mediated plant transformation. *Trends Plant Sci* 7(5):193–195.
5. Goderis IJ, et al. (2002) A set of modular plant transformation vectors allowing flexible insertion of up to six expression units. *Plant Mol Biol* 50(1):17–27.
6. Wise AA, Liu Z, Binns AN (2006) Three methods for the introduction of foreign DNA into *Agrobacterium*. *Methods Mol Biol* 343:43–53.
7. Clough SJ, Bent AF (1998) Floral dip: A simplified method for *Agrobacterium*-mediated transformation of *Arabidopsis thaliana*. *Plant J* 16(6):735–743.
8. Alexander MP (1969) Differential staining of aborted and nonaborted pollen. *Stain Technol* 44(3):117–122.
9. Qin Y, et al. (2009) Penetration of the stigma and style elicits a novel transcriptome in pollen tubes, pointing to genes critical for growth in a pistil. *PLoS Genet* 5(8): e1000621.
10. Qin Y, et al. (2011) Sulfinylated azadecalins act as functional mimics of a pollen germination stimulant in *Arabidopsis* pistils. *Plant J* 68(5):800–815.
11. Smyth DR, Bowman JL, Meyerowitz EM (1990) Early flower development in Arabidopsis. *Plant Cell* 2(8):755–767.

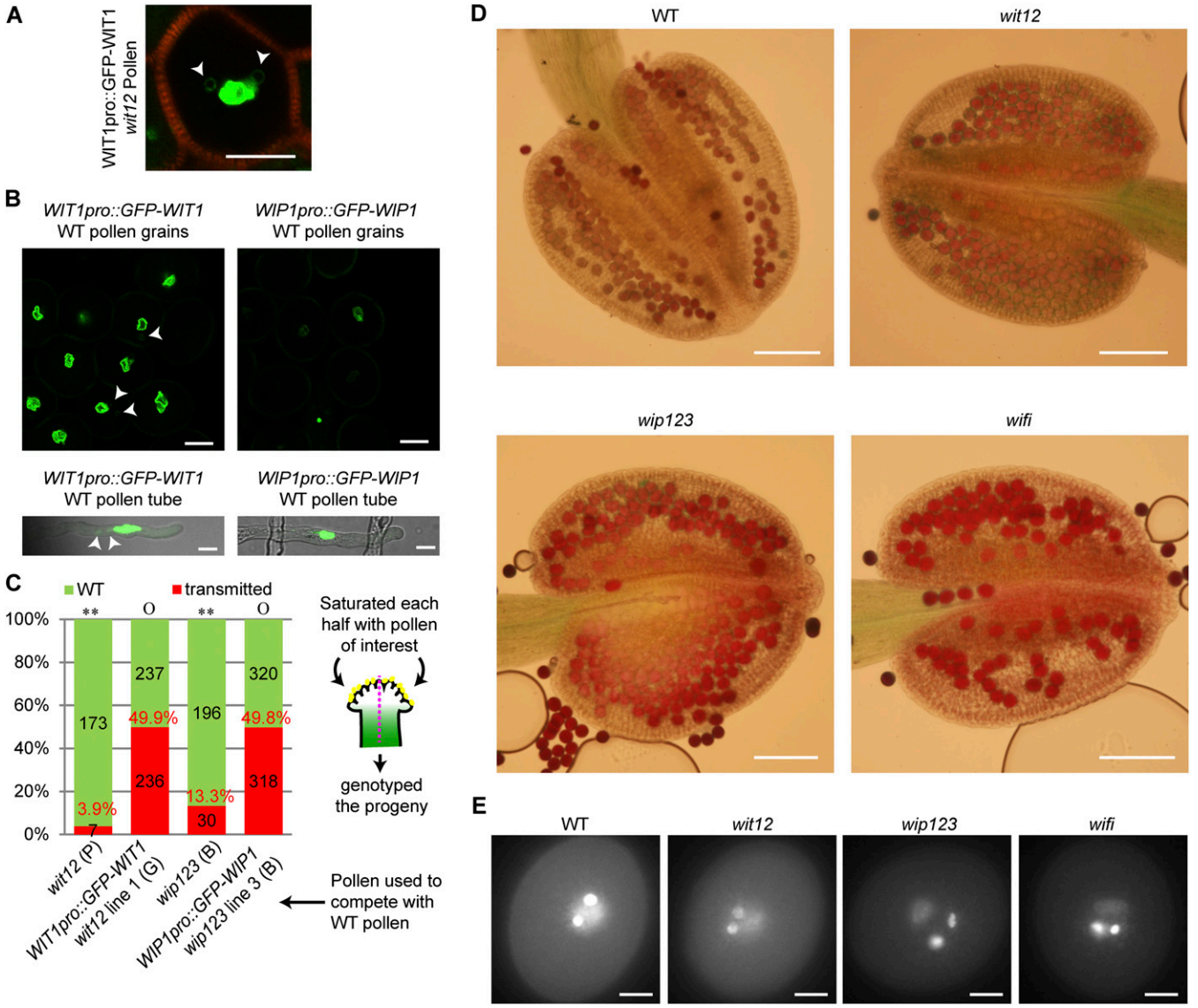

Fig. S1. Analysis of the function of WIT and WIP in pollen viability. (*A*) In a *WIT1pro::GFP-WIT1 wit1-1 wit2-1* double null (*wit12*) pollen grain, GFP-WIT1 strongly labeled the vegetative nuclear envelope (VNE) and weakly labeled the sperm cell (SC) nuclear envelope (NE; arrowheads). The imaging conditions were adjusted to view the SC NE, and the VNE GFP signal is saturated. (Scale bar: 10 μm.) (*B*) GFP-WIT1 was localized to the VNE in *WIT1pro::GFP-WIT1* WT pollen and pollen tubes, and GFP-WIP1 was localized to the VNE in *WIP1pro::GFP-WIP1* WT pollen and pollen tubes. GFP-WIT1 was also weakly expressed in the SCs and probably localized to the SC NE (arrowheads). The imaging conditions were adjusted to view the SC NE, and the VNE GFP signal is saturated. (Scale bars: 10 μm.) (*C*) Pollen competition assays were performed between WT pollen and (*i*) *wit12* pollen, (*ii*) *WIT1pro::GFP-WIT1 wit12* line 1 pollen, (*iii*) *wip1-1 wip2-1 wip3-1* triple null (*wip123*) pollen, and (*iv*) *WIP1pro::GFP-WIP1 wip123* line 3 pollen. As illustrated by the cartoon, one-half of a stage 14 WT stigma (1) was saturated with WT pollen, and the other one-half was saturated with the competing pollen. The genotype of the progeny was determined to calculate the transmission efficiency (number of progeny containing the mutant allele/total number of progeny). **Statistically significant difference to 50% efficiency ($P < 0.01$, two-tailed Fisher exact test). ^{O}No statistically significant difference ($P > 0.05$, two-tailed Fisher exact test). The observed number of each category is indicated in black, and the transmission efficiency is shown in red. Letters in parentheses represent the method used for genotyping: B, Basta resistance of the *wip123* genotype; G, GFP fluorescence; P, PCR amplification of the *wit2-1* allele. (*D*) Pollen grains were stained using Alexander's staining. No obvious dead pollen grains were found in *wit12*, *wip123*, and quintuple null mutant *wip1-1 wip2-1 wip3-1 wit1-1 wit2-1* (*wifi*). (Scale bars: 100 μm.) (*E*) Pollen grains were stained with Hoechst 33342. The three nuclei—one vegetative nucleus and two SC nuclei—were normal in the pollen grains of *wit12*, *wip123*, and *wifi*. (Scale bars: 5 μm.)

1. Smyth DR, Bowman JL, Meyerowitz EM (1990) Early flower development in Arabidopsis. *Plant Cell* 2(8):755–767.

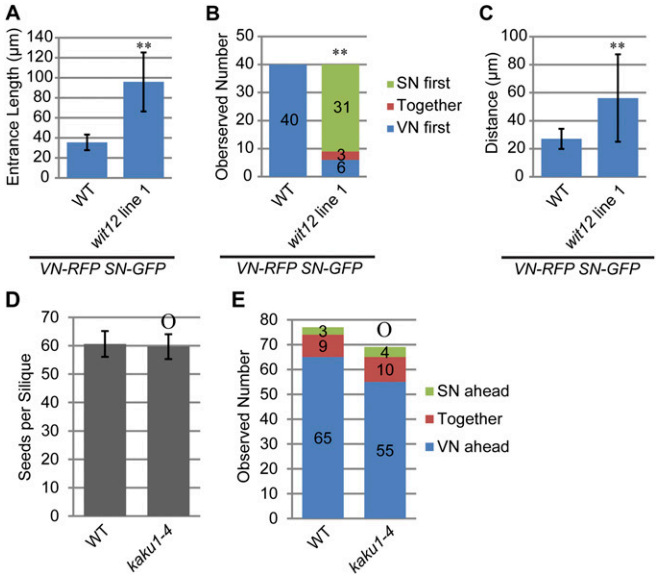

Fig. S2. Analysis of pollen tube growth of *wit1-1 wit2-1* double null (*wit12*) and *kaku1-4*. (*A*) Entrance lengths of WT and *wit12* pollen tubes. $^{**}P < 0.01$ compared with WT ($n = 40$, two-tailed *t* test). Error bars represent SD. SN, sperm cell nuclei; VN, vegetative nucleus. (*B*) First nucleus that entered the pollen tubes of WT and *wit12*. **Statistical significance compared with WT ($P < 0.01$, two-tailed Fisher exact test; numbers of each category are shown on the graph). (*C*) Distance between the leading nucleus and the pollen tube tip. The nuclear movement of 10 WT pollen tubes and 10 *wit12* pollen tubes was tracked every 1 min for 60 min, and the distance was the average of all tracking points. **Significance < 0.01 compared with WT ($n = 600$, two-tailed *t* test). Error bars represent SD. (*D*) A reported *myosin xi-i* mutant (1), *kaku1-4*, has normal seed number per silique. $^{O}P > 0.05$ compared with WT ($n = 40$, two-tailed *t* test). Error bars represent SD. (*E*) *kaku1-4* Has normal nuclear order in pollen tubes 5 h after in vitro pollen germination. $^{O}P > 0.05$ compared with WT (two-tailed Fisher exact test; the number of each category is shown on the graph).

1. Tamura K, et al. (2013) Myosin XI-i links the nuclear membrane to the cytoskeleton to control nuclear movement and shape in *Arabidopsis*. *Curr Biol* 23(18):1776–1781.

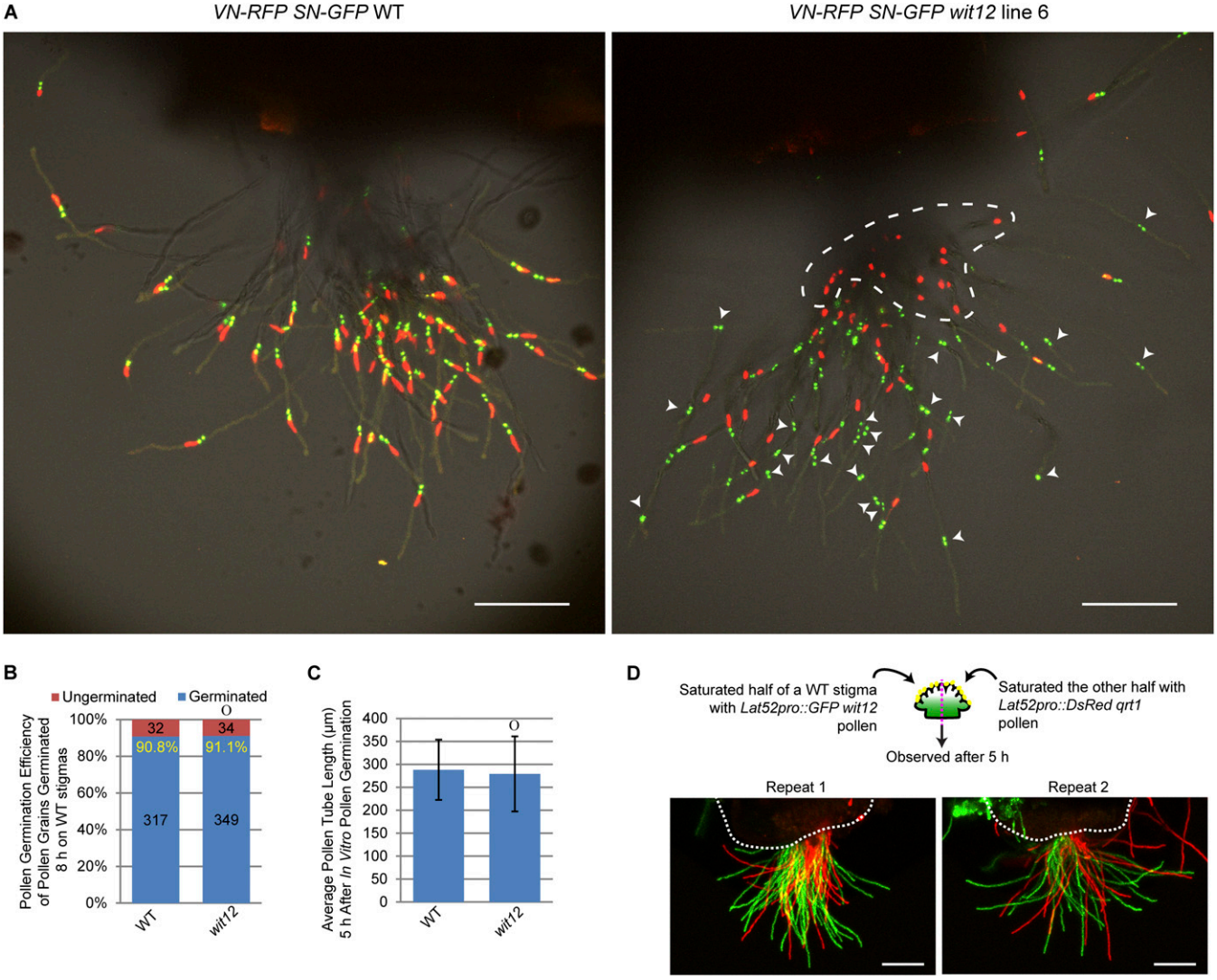

Fig. S3. Effects of *wit1-1 wit2-1* double null (*wit12*) mutation on pollen tube growth. (*A*) WT and *wit12* pollen grains carrying the *vegetative nucleus* (*VN*) *-RFP sperm cell nuclei* (*SN*) *-GFP* were simultaneously germinated on WT stigmas in the same pollen germination medium and imaged 8 h after semi-in vivo pollen germination. Nuclear position in the *wit12* pollen tubes was still reversed compared with WT. In addition, isolated VN (circled by the dotted line) and solely migrating SN pairs (arrowheads) were visible. For each image, a *z*-stack image was taken, and the maximum projections of the GFP and RFP channels were merged with a representative bright-field image. (Scale bars: 100 μm.) (*B*) *wit12* Mutation does not affect pollen germination efficiency (number of germinated pollen grains/total pollen grains observed). Pollen grains carrying *VN-RFP* and *SN-GFP* were used to pollinate stage 14 stigmas of the *male sterility 1* (*ms1*) mutant. Pollen grains were imaged 8 h later on the stigmas. Pollen grains without the VN-RFP and SN-GFP signals were considered germinated. The number of each category is indicated on the graph, and the germination efficiencies are shown in yellow. $^{O}P > 0.05$ compared with WT pollen grains (two-tailed Fisher exact test). (*C*) The *wit12* mutation does not affect pollen tube growth rate. WT and *wit12* pollen grains were germinated in vitro for 5 h before measurements. $^{O}P > 0.05$ compared with WT ($n = 120$, two-tailed *t* test). Error bars represent SD. (*D*) No overall pollen germination defects and pollen tube growth defects were observed when *wit12* pollen competed with *qrt1* pollen. One-half of a stage 14 *ms1* stigma was saturated with *Lat52pro::GFP wit12* pollen, and the other one-half was saturated with *Lat52pro::DsRed* (*DsRed* driven by the *Lat52 promoter*) *qrt1* pollen. Pollen tubes were imaged 5 h later, and two independent repeats were performed. Each image is a maximum projection of a *z*-stack image. The edge of each stigma is outlined by a dotted line. (Scale bars: 100 μm.)

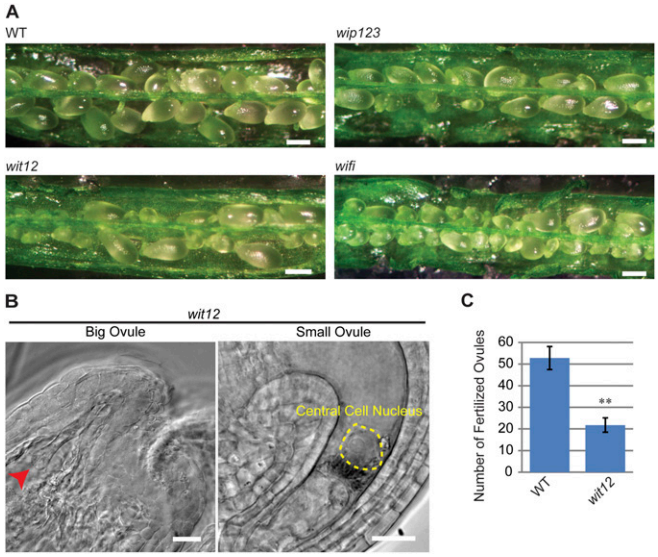

Fig. S4. Fertilization defects in *wit1-1 wit2-1* double null (*wit12*), *wip1-1 wip2-1 wip3-1* triple null (*wip123*), and quintuple null mutant *wip1-1 wip2-1 wip3-1 wit1-1 wit2-1* (*wifi*) ovules. (*A*) Large numbers of small ovules were found in *wit12*, *wip123*, and *wifi* ovaries ~72 h after flower opening compared with WT. (Scale bars: 200 μm.) (*B*) Large ovules contain a developing embryo (red arrowhead), whereas small ovules were not fertilized, which was indicated by a clear central cell nucleus (yellow dotted line). (Scale bars: 40 μm.) (*C*) *wit12* Had a statistically significantly reduced number of large fertilized ovules in ovaries ~72 h after flower opening compared with WT. Error bars represent SD. $^{**}P < 0.01$ ($n = 5$, two-tailed t test).

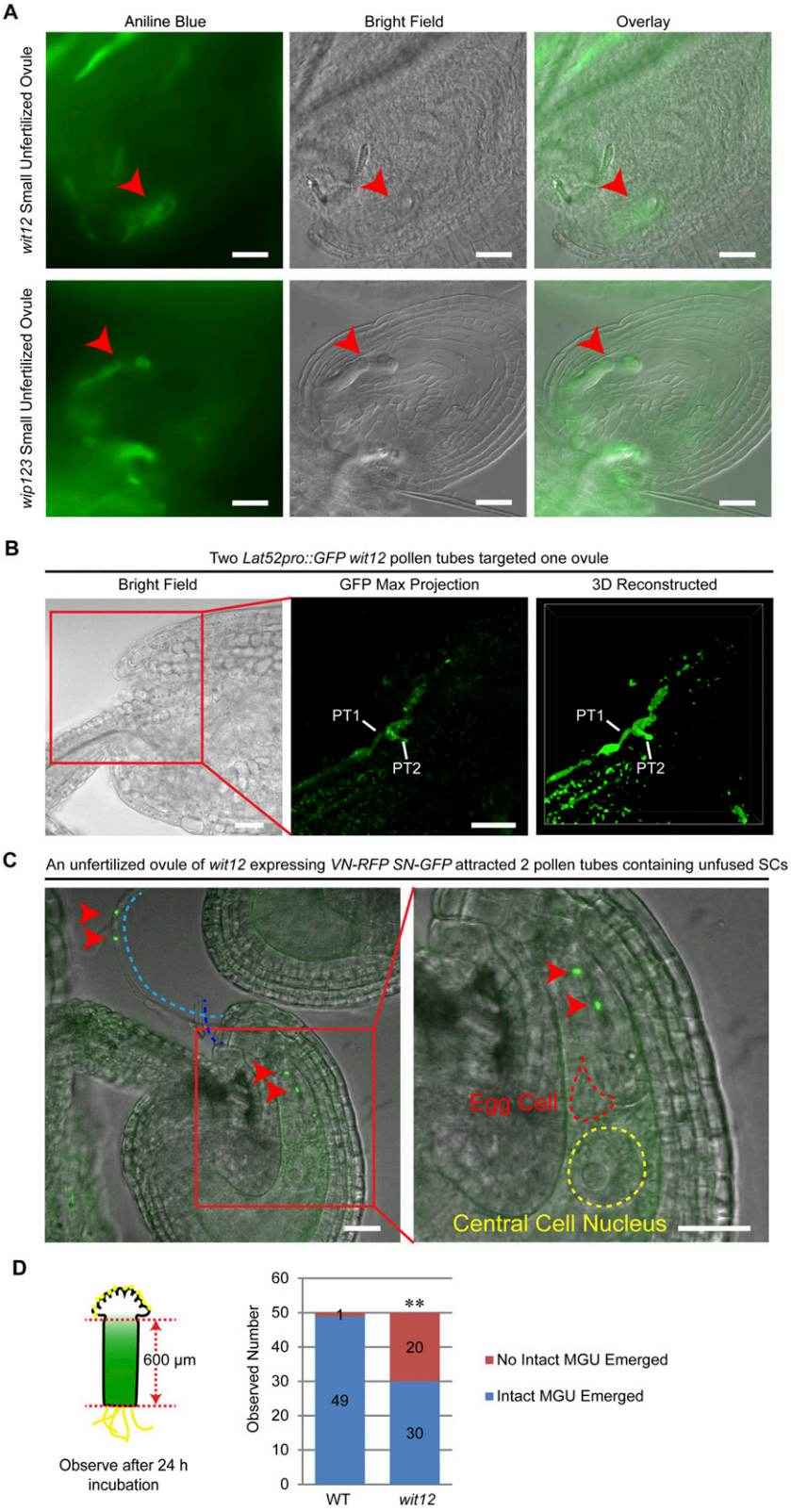

Fig. S5. Pollen tube reception and sperm cell (SC) -to-ovule migration defects of *wit1-1 wit2-1* double null (*wit12*). (*A*) The overgrown pollen tubes in *wit12* or *wip1-1 wip2-1 wip3-1* triple null (*wip123*) small unfertilized ovules were revealed by aniline blue staining. Arrowheads indicate the overgrown pollen tubes. (Scale bars: 20 μm.) (*B*) Two *Lat52pro::GFP wit12* pollen tubes targeted one ovule. *Left* is a bright-field image showing the overview of the ovule. A maximum projection of the GFP signal present in the area framed by the red frame is enlarged and shown in *Center*. *Right* is a 3D reconstruction image of the same *z*-stack image using α-blending. To reduce noise, a 5-pixel median filter was used. PT1, pollen tube 1; PT2, pollen tube 2. (Scale bars: 20 μm.) (*C*) Positions of the

Legend continued on following page

SC nuclei (SN) in pollen tubes targeted a small unfertilized ovule of *vegetative nucleus* (*VN*) *-RFP SN-GFP wit12*. In *Left*, cyan and blue dotted lines mark the two pollen tubes that targeted the ovule. The area in the red frame is enlarged in *Right*, where an egg cell (red dotted line) and a central cell nucleus (yellow dotted line) are visible. Arrowheads indicate the SN. (Scale bars: 20 μm.) The SN-GFP signal is a maximum projection of a *z*-stack image, which was processed with a 1-pixel median filter to reduce noise and overlaid with a representative bright-field image. (*D*) The VN was disconnected in a large number of in vivo-grown *wit12* pollen tubes. Stage 14 *male sterility 1* pistils were pollinated with *VN-RFP SN-GFP* WT or *VN-RFP SN-GFP wit12* pollen. These pistils were then cut to have ovaries ~600 μm in length (illustrated by the cartoon) and incubated on a pollen germination medium for 24 h. Pollen tubes that grew through these pistils were examined. Pollen tubes with both the VN and the SCs detectable within 250 μm from the pollen tube tip were considered as intact male germ unit (MGU) emerged; otherwise, they were considered as no intact MGU emerged. The number of each category is indicated on the graph. $^{**}P < 0.01$ compared with WT (two-tailed Fisher exact test).

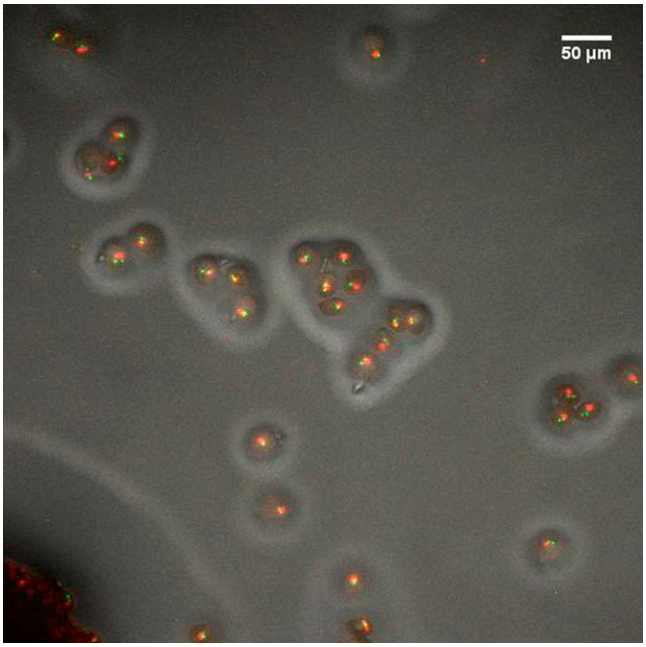

Movie S1. Nuclear movement in WT pollen grains germinated in vitro. A 600× speed playback of WT pollen grains germinated in vitro for 180 min. The vegetative nucleus (red) and sperm cell nuclei (green) were tracked every 1 min.

Movie S1

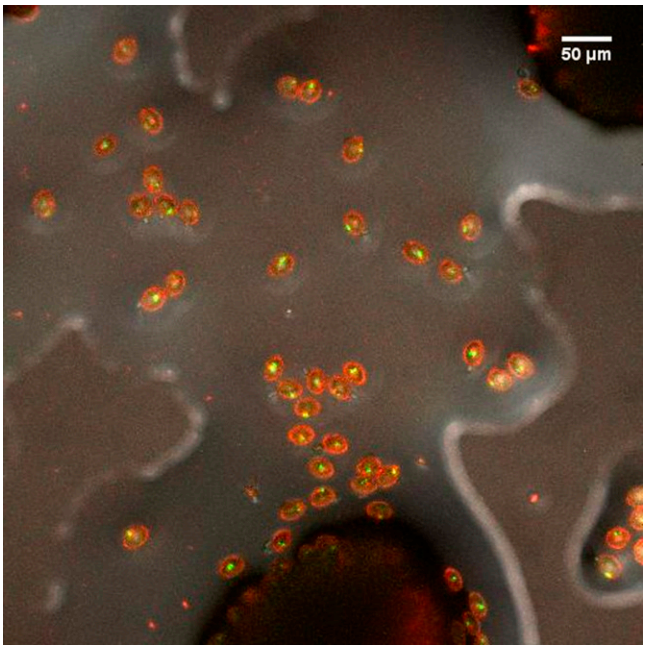

Movie S2. Nuclear movement in *wit1-1 wit2-1* double null (*wit12*) pollen grains germinated in vitro. A 600× speed playback of *wit12* pollen grains germinated in vitro for 180 min. The vegetative nucleus (red) and sperm cell nuclei (green) were tracked every 1 min.

Movie S2